and the 20 percent uncertainty in $\Delta\nu_0$ rendered the value of A thus obtained too inaccurate for satisfactory check. Additional data were taken in which the pressure variation during a run was reduced to a negligible amount, and values of $\Delta\nu_0$ showing variations of less than 10 percent were obtained. From these data a value of $A=(1.6\pm0.3)\times10^7$ cm^2/erg sec. was calculated, agreeing with the theoretical value when Zeeman averaging is included.

PHYSICAL REVIEW VOLUME 73, NUMBER 9 MAY 1, 1948

Secondary Electron Emission from Targets of Barium-Strontium Oxide

J. B. JOHNSON
Bell Telephone Laboratories, Incorporated, Murray Hill, New Jersey
(Received December 22, 1947)

The secondary electron yield of (BaSr)O has been studied, as induced by microsecond pulses of primary electrons with energy up to 2000 ev. The δ *vs.* V_p curves have the usual form, with maximum δ near 1200 ev. At room temperature, and before surface charges build up, the δ_{max} is of the order 12, but it may be reduced to 6 by less than 0.1 atomic layer of Ba evaporated from a nearby thermionic cathode. With increasing temperature δ decreases to an apparent minimum at ~600°C. With the onset of d.c. thermionic emission the total yield increases during each pulse, in rough proportion to the thermionic current. The increase is thought to represent a transient change in thermionic activity caused by the bombardment. No change with temperature is observed for the energy distribution of the true secondaries. The possibility of field-enhanced secondary emission at low temperatures is considered.

I. INTRODUCTION

IN earlier short notes and abstracts some results of pulsed measurements on the secondary emission properties of thermionic oxide cathodes were described.[1] Briefly, the results were these: The yield δ of secondary electrons from oxide cathodes is relatively high, from 4 to 10 at the optimum voltage, depending on various conditions. Near room temperature the δ tends to be high, decreasing slowly with temperature up to 600°C. In the temperature region where thermionic emission is appreciable, an increase in the thermionic emission occurs during and shortly after the bombardment with primary electrons and this emission is superimposed on the secondary current.

These measurements have now been amplified and extended and will be described more fully in this paper. The earlier conclusions are supported in all essentials, particularly as regards the presence of the bombardment-enhanced thermionic emission. The principal results of the measurements on secondary emission are given in Section 4.0 of the paper, which deals with the influence of the various parameters such as primary energy, temperature, current density, and other factors on the secondary emission ratio of the oxide target. The test circuit and the general characteristics of the experimental tubes are dealt with in Section 2.0. In Section 3.0 are described the specific characteristics of a particular tube and target from which the typical results in Section 4.0 were derived, involving the determination of temperature, thermionic activity, and the possible limitations imposed on the measurements by space charge in the tube. Matters which do not bear directly on the main results of Section 4.0 but which are still of considerable interest are dealt with in the last four sections. These include the effects of barium poisoning, the primary energy at which $\delta=1$, the energy of the secondary electrons, and the possible effects of high internal field in the target.

Two other reports on the secondary yield of oxide cathodes have appeared in recent years. The first, by Morgulis and Nagorsky,[2] presents

[1] J. B. Johnson, Phys. Rev. 66, 352 (1944); Phys. Rev. 69, 693 (1946); Phys. Rev. 69, 702 (1946).

evidence obtained by a d.c. method that the secondary yield from the oxide cathode increases exponentially with temperature from its room temperature value to the point where the secondary emission is eventually swamped by the thermionic emission. Later work by Pomerantz,[3] using in part a technique of microsecond pulsing very similar to that of the present work, supports the conclusions of Morgulis and Nagorsky. Extrapolation to higher temperatures indicated that a very high secondary yield should be reached. In the work to be reported on here the results and interpretations differ in several respects from those of the other authors, and are therefore presented in considerable detail.

II. APPARATUS

2.1 Tube Structure

In order to have a set of consistent data, nearly all of the experiments reported here have been made on a single tube, MN-74. All of the phenomena have been observed on other tubes, so that they are not peculiar to this one specimen of tube or target, but in the present tube the target is even closer to the collector electrode than in previous tubes, in order to reduce the effect of space charge. Figure 1 shows a scale drawing of part of the tube, with electron gun, the two perforated copper disks serving as anode and collector, and the oxide-coated nickel cup serving as the target. The gun has a cathode with a standard oxide coating on grade A nickel, indirect heater, and a cap serving as grid for turning the electron beam on and off. The gun was designed by Dr. A. L. Samuel for another purpose, on the basis that the electron beam would have a cross-over near the gap between the copper disks independent of voltage between cathode and anode over a wide range. The target is a cup of grade A nickel $\frac{1}{4}$-inch in diameter. It is coated on the flat face with the standard "double carbonate"[4] coating of $(BaSr)CO_3$ about 0.001 in. thick. In pumping, the tube was baked at about 500°C, the electrodes were well outgassed with high frequency, the cathodes activated, the KIC getter fired, and the tube sealed off.

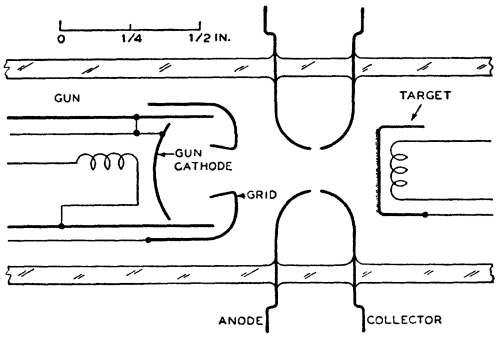

FIG. 1. Tube structure.

2.2 The Circuit

The testing circuit for pulsed operation is shown schematically in Fig. 2. The gun cathode is run at a potential V_p negative to ground in the range 0–2000 volts. Normally the gun is biased beyond cut-off, but is turned on by pulses of positive voltage from the pulser P, smoothly adjustable in voltage, and variable in duration from about 0.2 to 30 microseconds with a repetition rate to 500 to 4000 pulses per second. The collector is at the potential V_c, the gun anode is at +22 volts with respect to the collector to keep secondaries from the anode out of the collector space. For measuring the primary electron current, i_p, the target is made 22 volts more positive than the collector as shown in the diagram. The primary electrons then strike the target with energy which exceeds V_p by V_c+22 volts. This increase in energy does not alter the primary current appreciably and therefore makes no essential difference in the measurements. The effect of high energy secondaries which escape

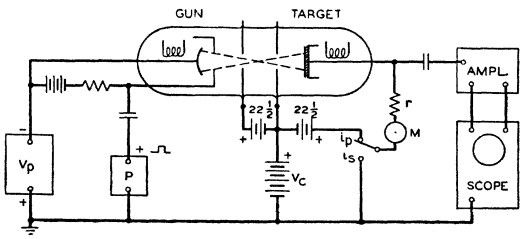

FIG. 2. Secondary emission circuit.

[2] N. Morgulis and A. Nagorsky, J. Tech. Phys. U.S.S.R. 5, 848 (1938).
[3] M. A. Pomerantz, J. Frank. Inst. **241**, 414 (1946); *ibid.* **242**, 41 (1946); Phys. Rev. **70**, 33 (1946).
[4] 45 percent $BaCO_3$, 55 percent $SrCO_3$, by weight, suspended in amyl acetate with a nitrocellulose binder.

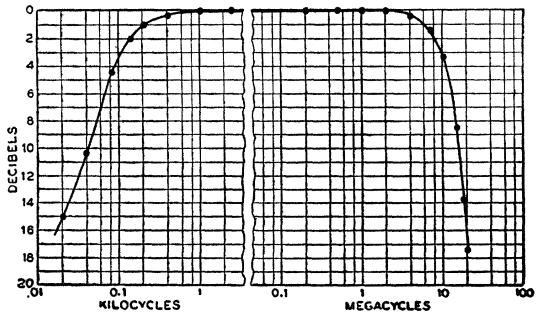

FIG. 3. Amplifier characteristic.

the target against the retarding potential of 22 volts, and so affect the measurement of the primary current, will be discussed later. When with the key in the position i_s the target is connected effectively to ground, the a.c. circuit measures the excess secondary current $i_s - i_p$, while the average d.c. current including any thermionic current i_{th} is measured by the d.c. meter. The electrons then strike the target with energy V_p, and the collector is positive by the amount V_c to draw the secondary electrons from the target. The target connection includes the load resistance r of 240 ohms, and a meter so that direct current in the target circuit can be measured. By-pass condensers are provided wherever needed in the circuit, but are not individually shown in the drawing.

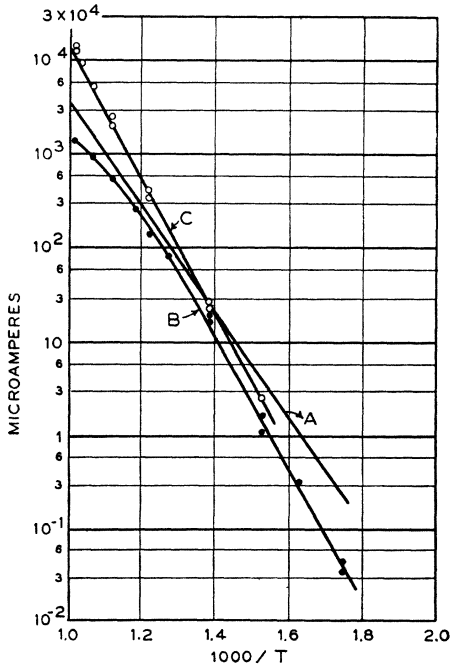

FIG. 4. Richardson plots of target: A—early, average, $V_c = 39$; B—late, $V_c = 6$; C—late, pulsed, $V_c = 36$.

The pulsed component of the target current is amplified and displayed on the oscilloscope. The amplifier has a flat characteristic that is down 3 db at a few hundred cycles and at 10 megacycles, about as shown in Fig. 3. It terminates in a balanced 829B tube that is resistance-capacity coupled to the plates of the 5LP1 cathode-ray tube. Its gain is such that 21μa in the target circuit gives 1.0-in. deflection on the scope at the highest gain. The gain is variable in six steps of 2.0:1.0.

The linear sweep circuit is coupled to the horizontal plates of the CR tube. The pulser, sweep, and intensity control are triggered by a synchronizer having adjustable repetition rate and phase.

III. CHARACTERISTICS OF TUBE MN-74

3.1 Temperature Calibration

For calibrating the temperature of the target a second tube was used containing only a target with as nearly as possible the same structure as that in MN-74. This target had welded to the center of its face a thermocouple of 0.003-in. Pt-PtRh wires for measurements in the low temperature range. The couple was calibrated against a mercury thermometer with the whole tube in an oven. For the high temperature range, the temperature of the target was measured by an accurate optical pyrometer, correcting for spectral emissivity of the target (taken as 0.40) and for the measured transmission of the slightly darkened glass wall (0.56). The heater power was the variable parameter in these calibrations, and the same calibrations were then assumed to hold for the target of MN-74 on the basis of equal heater power. The heater of this target was then calibrated in terms of a high resistance a.c. voltmeter which served as the indicating instrument during the tests. The temperature is probably not in error by as much as 20° in any part of the curve.

3.2 Thermionic Activity

The variation of thermionic emission of the target with temperature is shown by the Richardson plots of Fig. 4. The thermionic current

emitted from the 0.317 cm² of target area is plotted on a log scale, against 1000/T°K on a linear scale. Three experimental curves are shown: (*A*) an extensive set of readings made early in the life of the tube, with $V_c = 39$ volts; (*B*) a set made toward the end of the present tests, with V_c at 6 volts; and (*C*) a set made at the same period as *B* but with the initial current read on the 'scope as V_c of 36 volts was applied by the tap of a key. In *B*, as contrasted with *C*, the effect of decaying emission with time after applying V_c is clearly shown, especially at the higher temperatures. When δ-measurements are made the V_c has always been on for several seconds so that the lower lying curves should then more nearly apply. The thermionic currents were not extrapolated to the values for zero field by means of the log *i vs.* $E^{\frac{1}{2}}$ plot as is sometimes done. The curves show that there was a change of thermionic constants toward lower activity during the course of the tests.

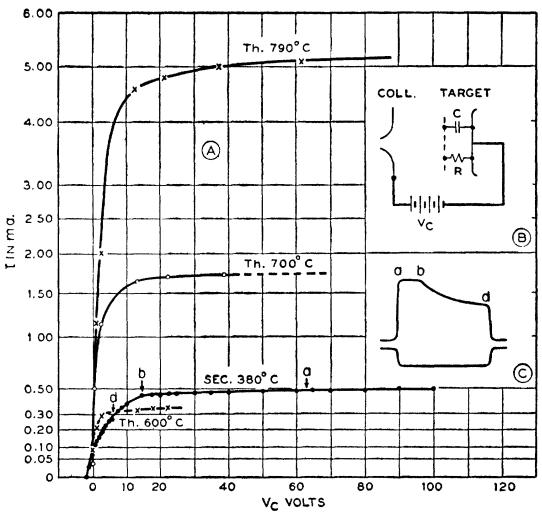

FIG. 5. Current-voltage curves, and effect of surface charge. Currents on $\frac{2}{3}$-power scale. *A*—thermionic current at 600°, 700°, 790°C. Secondary current at 380°C. Space charge limitation at lower values of collector potential V_c. *B* and *C*, discussed in text.

3.3 Space Charge Conditions

In Fig. 5A are shown curves for electron emission from the target as a function of collector voltage V_c. The currents are plotted on a $\frac{2}{3}$-power scale. The steep parts of the curves define regions where the current is limited by space charge. A log *i vs.* $E^{\frac{1}{2}}$ plot of the more nearly horizontal parts of the curves yields nearly straight lines, showing that here space charge limitation is not significant. The curves marked Th correspond to d.c. thermionic emission at the temperatures 600°, 700°, and 790°C. In the subsequent tests the thermionic emission was never larger than the highest of these, and the collector potential was usually 63 volts. The curve marked Sec. was made with pulsed secondary emission current at the temperature 380°C where the thermionic current was negligible and the secondary pulse was flat-topped. This current of 0.5 ma is larger than ever used in the δ-tests. With the aid of these curves it was arranged that space charge was never a serious limitation upon either thermionic or secondary measurements.

IV. SECONDARY EMISSION MEASUREMENTS

4.1 Procedure

The measurements of secondary yields will be described with the aid of Fig. 8, which is a series of photographs* of the patterns on the 'scope, made at various target temperatures. The pattern for 400°C may be selected. The lower trace represents a pulse of primary current set to read 0.40 in. on the screen, which corresponds to 8.5-μa beam current. The collector is 22-volts negative. Time passes from left to right and the pulse is 4.0μsec. long. The upper trace, with the axis shifted upward slightly to prevent overlap in the photograph, is the corresponding secondary current, the collector being here 63-volts positive. The gain of the amplifier is reduced by a factor 4.0 for this trace in order to keep the two traces at nearly the same size. The pulse rate was 1000 per second, with each photograph exposed here 3 seconds.

Normally the readings were made directly on the 'scope by means of an accurate reticle in front of the screen, rather than from photographs The primary pulse was set usually to give the primary deflection $D_p = 0.40$ in. by adjusting the pulser output, at some selected amplifier gain. The gain was then decreased by a factor 4.0 and the height of the secondary pulse D_s was

* In the original negatives of these oscillograms the steep side-traces are clearly visible but are too faint to reproduce in the printing. These parts have therefore been intensified without any of their features being altered.

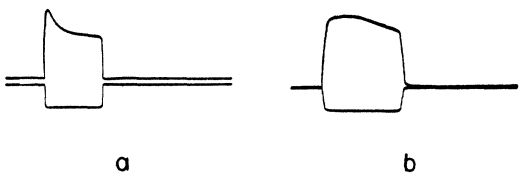

FIG. 6. Charging of target surface. $V_p=1250$; $V_c=63$; $T=30°C$; $i_p=34$ μa; a, $t=10$ μsec.; b, $t=2$ μsec.

observed, giving the yield almost directly:

$$\delta=\frac{4D_s+D_p}{D_p}=\frac{4D_s}{D_p}+1=\frac{4D_s}{0.4}+1=10D_s+1.$$

In the figure just considered δ is thus 8.2. The remaining photographs of Fig. 8 were made with the target at different temperatures but otherwise under constant conditions.

The δ so measured is subject to the limitations that not all the secondaries are stopped by the retarding potential of 22 volts, and that the secondary current does not saturate sharply but varies somewhat with collector voltage as is shown later in Figs. 21–22. These conditions form part of the definition of the present δ.

4.2 δ at Low Temperatures, and the Charging Effect

At room temperature, Fig. 8, the secondary pulse is seen to reach a maximum value quickly and then to decrease with time. This is shown more clearly in Fig. 6, where the curves were made with larger beam current and with two different pulse lengths. In Fig. 6a the pulse length is 10 μsec. and a slow sweep is used, while in 6b details of the early part of the pulse are shown using a faster sweep and a 2 μsec. pulse under otherwise identical conditions. This shape of the secondary pulse arises from the fact that the coating is at this temperature a fair insulator and its surface charges positive under the bombardment when δ is greater than one.

The effect is illustrated by the curves of Fig. 5. In Fig. 5B the oxide coating is drawn as having resistance R and capacity C per unit area, between the outer surface and the base, with the potential V_c between base and collector. Initially the surface is at the same potential as the base and conditions are as indicated at a in Fig. 5A and 5C. As now an excess of electrons flows from the surface to the collector the capacity becomes charged, reducing the effective collector voltage until it can no longer support the full secondary current. The surface potential is then within a few volts of the collector potential and the current breaks as at b in Fig. 5A and 5C. The current finally decreases to an equilibrium value where it is limited chiefly by the iR drop in the coating as at d in the figures. The time from the beginning of the pulse to the point where the decrease begins, about 0.8 μsec. in Fig. 6b, is nearly proportional to V_c, and varies in not quite the inverse proportion with the beam current.

In this temperature range, then, the measure of δ is taken from the peak height of the secondary pulse. The curves of Fig. 8 show that the charging effect disappears rapidly as the temperature, and with it the conductivity, of the target increases. At the same time the peak height of the pulse decreases so that δ becomes less with increasing temperature.

The charging effect and the high values of δ at low temperatures could not have been observed in the d.c. method of Morgulis and Nagorsky, and were not found by Pomerantz. Possibly in the latter case the resistance of the coating was for some reason never as high as here, or the bombarded area was larger. It is not known whether the accumulation of charge and the high δ are related, but it seems quite possible either on the basis that secondary electron escape more readily from an insulator than from a better conductor[5] or that in the insulator internal fields are set up which direct the secondaries toward the outside.[6] Of the reality of the charging effect there is no question.

4.3 The Bombarded Area

The size of the target area bombarded by the beam of primary electrons needs to be known for some of the results which are to be cited. It cannot be seen directly by the fluorescence of the coating, but the charging effect gives a

[5] H. Bruining and H. J. deBoer, Physica 6, 823 (1939); G. Maurer, Zeits. f. Physik 118, 122 (1941); H. Bethe, Phys. Rev. 59, 940 (1941).

[6] H. Hintenberger, Zeits. f. Physik 114, 98 (1939); H. Bruining and H. J. deBoer, Physica 6, 823 (1939); P. V. Timofeef and R. M. Aranovich, J. Tech. Phys. U.S.S.R. 10, 32 (1940); D. V. Zernov, Bull. Acad. Sc. U.S.S.R. 8, 352 (1944).

method of estimating this area. At the point of break, as at b in Fig. 5A and 5C, the total charge on the bombarded area σ_s is

$$q=(i_s-i_p)t_b=C\sigma_s(V_a-V_b),$$

where (i_s-i_p) is the excess of secondary over primary current, t_b the time at break, V_a the initial value of collector voltage, and V_b the effective collector potential at break, usually estimated at a few volts, and C is the capacitance per cm² of the coating. (The resistance R plays only a minor role up to this stage of the process.)

For determining C, the target from another tube, similarly activated, was removed and the capacity between the base and a plate pressed lightly against the oxide was measured, with suitable precautions. It was 51 $\mu\mu$f, the capacitance C of the coating[7] being then 160 $\mu\mu$f per cm². The extent of the bombarded area σ_s was computed from a series of measurements with varied i_p and V_c, for a fixed V_p of 1250. The results are shown in Fig. 7, where σ_s is given as a function of i_p. The curve covers the whole range of beam currents used, and σ_s is always small compared to the total area of the target. The area ought not to vary in any major way with V_p.

Another method of estimating the area is furnished by the current-voltage curves of Fig. 5A, where saturation of the curve of secondary current may be compared with that for the nearly equal thermionic current at 600°C. The secondary current requires higher V_c for saturation than thermionic current of the same magnitude. This is because only a small part of the target area is bombarded by the primary electrons whereas the thermionic current comes from the whole area. A comparison of the secondary curve and the lowest thermionic curve gives a rough estimate of the area on which the primary beam impinges. Neglecting initial velocities and assuming the $\frac{3}{2}$-power law to hold, we have

$$\frac{\sigma_s}{\sigma_t}=\frac{i_s}{i_t}\left(\frac{V_t}{V_s}\right)^{\frac{3}{2}},$$

where t refers to thermionic and s to secondary

[7] The measured thickness of the coating was 0.0008 in., density 1.27, dielectric constant 3.5 at the frequency of one megacycle.

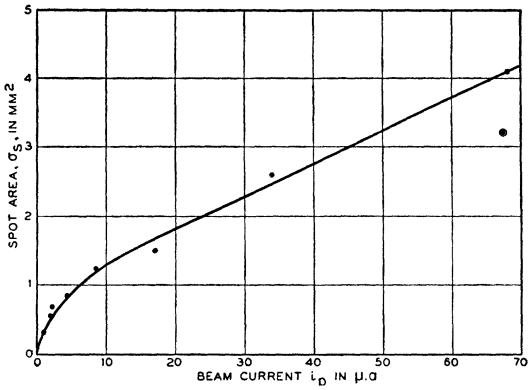

FIG. 7. Variation of spot area with beam current. $V_p=1250$. Total target area, 31.7 mm².

currents and the V's refer to saturation voltages. The total area is $\sigma_t=0.317$ cm². Values may be taken from the curves as follows: $V_t=2.5$, $V_s=15$ volts; $i_t=0.30$ ma, $i_s=0.45$ ma. This gives for the bombarded area $\sigma_s=0.032$ cm², when the primary beam current was 68 μa at 1250 volts. The large point in Fig. 7 represents this value, and it is not much out of line with the other points of the figure.

4.4 δ at Higher Temperatures, and the Bombardment-Enhanced Thermionic Emission

Returning to Fig. 8, we see that above 650°C the shape of the secondary pulse departs in a different way from that of the primary one. The charging effect has ceased, D_s rises during the pulse, and a tail remains at the end of the pulse. At the same time, thermionic current is emitted by the target and is measured separately by the d.c. meter but it does not directly appear in the

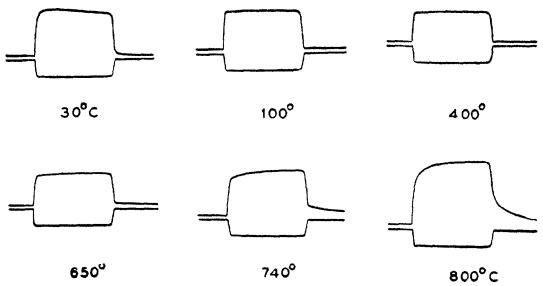

FIG. 8. Variation of yield with temperature. Lower trace, primary current; upper trace, secondary current on $\frac{1}{4}$-scale. Base lines separated by vertical shift on 'scope. Pulse time $t=4$ μsec., from left to right. $i_p=8.5$ μa; $V_p=1250$.

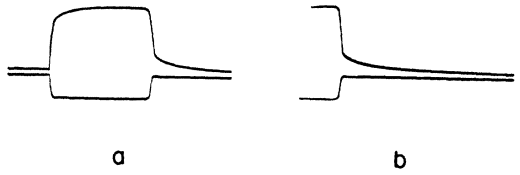

FIG. 9. Enhanced thermionic emission curves. $V_p=1250$; $T=800°C$; $i_p=17$ μa; $t=4$ μsec. Curves b are the same as a, but shifted to left to show more of tail.

D_s. In Fig. 9 the tail of a pulse is followed for a longer time.

The current that produces the tail flows after the primary pulse is over and cannot be secondary current.[8] It must be a temporary increase in the thermionic current, and presumably the increase in current *during* the pulse must be of the same origin. The emission is not caused by local heating at the surface of the target, for calculations show conclusively that heating by the bombardment must be quite negligible. Some part of the secondary emission process, rather, must change temporarily the thermionic constants of the target. An increase in the number of conduction electrons under the bombarded surface could raise the thermionic emission, though the validity of this mechanism could not be urged without careful study.

At low temperatures the δ is seen, as in Fig. 8, to decrease with increasing temperature. In the higher temperature range it becomes difficult to select by inspection the boundary between secondary emission and the added thermionic emission and to say how much each contributes to the final pulse height. Attempts were made to find the boundary by making semilog plots of the top or tail of pulses on the basis that they might be exponential with a definite intercept at zero time.

Such plots are shown in Fig. 10 for the top and tail of the pulse in Fig. 9 as measured on the photographic film. If the pulse top can be represented by the time function

$$D_s=D_0+D_1(1-e^{-\alpha t})$$

or

$$D_0+D_1-D_s=D_1e^{-\alpha t}=y,$$

then y should have an intercept D_0 when the curve is extrapolated to $t=0$. Curve A of Fig. 10 is such a plot for the head of the pulse. At long times the curve represents an exponential with a time constant of about 0.67 μsec. and an intercept at 0.35 in. below the top at 1.13 in. as measured on the 'scope. This suggests that the true secondary emission is given by

$$\delta_0=10(1.13-0.35)+1=8.8.$$

On the other hand, the point at 0.1 μsec. is definitely out of line and points to a higher intercept and lower δ_0. This is at the limit of resolution of the system so that one cannot say with certainty where the intercept actually is. A similar graph for the tail of the pulse is given by B of Fig. 10. Here the curve may represent two exponentials, one certainly with a longer time constant. The intercept may again be at 0.35 in., but the 0.1-μsec. point suggests a higher one. A number of such curves plotted for different conditions have failed to make a clear separation and thus to show how the true δ varies with temperature in the region of the enhanced thermionic emission. It may be that the curves are not truly exponential, or that higher time resolution is needed.

For the purpose of the next figure, in view of this difficulty, the highest yield during a pulse

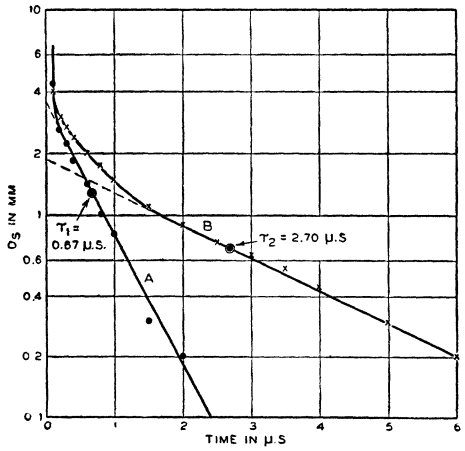

FIG. 10. Time constants and intercepts of head (A) and tail (B) of enhanced emission. Plotted from photograph. $V_p=1250$; $T=800°C$.

[8] The interval between the arrival of a primary electron and the emission of the secondaries has been estimated as follows: (4×10^{-10} sec.), F. Kirchner, Ann. d. Physik **78**, 277 (1925). Less than 2×10^{-9} sec., L. Malter, Proc. I.R.E. **29**, 578 (1941); for at least some electrons less than 5×10^{-11} sec., M. H. Greenblatt and R. H. Miller, Jr., Phys. Rev. **72**, 160 (1947).

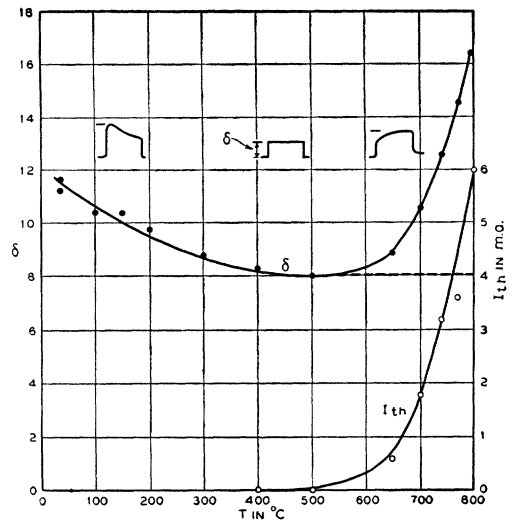

FIG. 11. Variation of yield δ with temperature. Inserts show shape of secondary current pulse for the various regions, for defining δ. $\delta_{min}=8.0$; $V_p=1250$; $i_p=8.5$ μa. D.c. thermionic current shown as I_{th}.

will be called δ. In Fig. 11 are plotted the yields given by the series of photographs from which those of Fig. 8 were selected, against target temperature. Many such runs have been made. They differ slightly one from the other but the general features are the same. The yield definitely decreases with increasing temperature until appreciable d.c. thermionic emission sets in, and then it increases rapidly. The curve I_{th} of Fig. 11 gives the thermionic current read at each time the corresponding photograph was made.

For a measure of the enhanced emission one needs to know how much of the yield is of true secondary origin. Figure 11 suggests that the true δ could continue to decrease with temperature, and the intercept extrapolations discussed above point rather to a slow increase. One expedient is to assume that δ remains constant at its minimum value, as suggested by the dashed line of Fig. 11, and to measure the increase from this value. A similar procedure was followed both by Morgulis and Nagorsky and by Pomerantz, with the minimum δ at room temperature, and they concluded that the increase in δ depends on temperature in the same way as does thermionic emission.

Data of this kind are plotted in Fig. 12. The independent variable is the current density of d.c. thermionic emission from the whole of the target, in ma/cm^2. The ordinates are the values of enhanced current density determined as in Fig. 11 by the difference between dashed and solid curves, with the bombarded area obtained in each case from Fig. 7. The bombarding primary current density is given by the circled points. Four different runs are included. While the points scatter somewhat, they lie along a band with 45° slope on the logarithmic scales, indicating proportionality between enhanced and steady-state thermionic emission. Over most of the range the density of bombarding current is small compared to either the steady or the enhanced emission, and for these particular conditions of primary voltage and current density the enhanced emission has about one-third the density of the steady thermionic emission.

4.5 Enhanced *vs.* Primary Current

The variation of enhanced thermionic emission with bombarding current is illustrated in Fig. 13. The four photographs were made with successively doubled beam current, reducing at the same time the gain in steps of 2.0. The curves superimpose with almost perfect fit, indicating that the enhanced emission is proportional to the bombarding current. Inspection of Fig. 7 shows that changing the current by the factor 8 changes the bombarded area by the factor 4 and therefore the current density by the factor 2.

4.6 Enhanced Current *vs.* Primary Voltage

The bombarding voltage is shown in Fig. 14 to have little effect on the enhanced emission

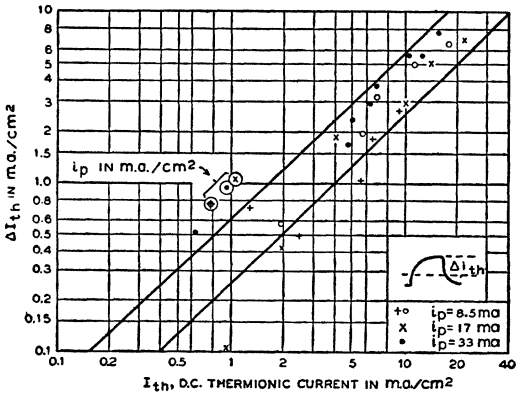

FIG. 12. Relation between normal and enhanced thermionic emission. ΔI_{th} is determined as $\delta-\delta_{min}$, as in Fig. 11. $V_p=1250$.

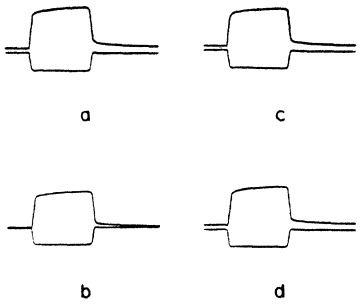

FIG. 13. Variation of enhanced emission with primary current. $V_p=1250$; $T=750°C$; $t=3$ μsec.; $i_p=a$, 8.5 μa; b, 17 μa; c, 34 μa; d, 68 μa.

over a considerable range, in agreement with the conclusion of Morgulis and Nagorsky. The photographs cover the range of V_p from 2000 volts down to 50 volts. Above 200 volts the tops of the secondary pulses are surprisingly alike, although the total heights of the pulses change considerably. This suggests strongly that in this region the true secondary yield increases rapidly with V_p while the enhanced thermionic emission remains constant, and that the two yields are fundamentally different. Below 200 volts the tops of the pulses become somewhat flatter and at 50 volts the enhanced emission appears rather small.

These findings are somewhat different from those of the earlier notes[1] where the enhanced emission seemed to vary somewhat less rapidly than the first power of the voltage and as the square root of the beam current. The characteristics of both the pulse and the amplifier were then such as to introduce an apparent, sharper but false boundary between secondary and thermionic yield. The present results with the improved system are thought to be in closer accord with the true facts.

4.7 Comparison with Pomerantz

The view taken here is that true secondary emission does not increase with temperature, but that the increased current is caused by a temporary change in the thermionic constants of the oxide cathode. Pomerantz, on the other hand, finds the steeply rising yield with temperature without evidence of the delayed rise and fall of the pulse at high temperatures, and his increased yield is evident even at temperatures too low for thermionic emission. In special cases he observed the rising head and falling tail, but he supposed them to be the spurious result of space charge or other neglected factors. Assuming that in both studies the space charge problem has been adequately considered, one must conclude that the targets of the two series of measurements were somehow different although they were intended to represent about the same kind of thermionic cathode. If in the targets of Pomerantz the large yield at high temperatures is caused by enhanced thermionic emission, then this enhancement must rise and fall in a time usually too short for the time resolution of his system. If, on the other hand, in the present work there is a rise of true secondary emission in the higher temperature range, it is not large enough to be distinguished clearly from the undoubted enhanced thermionic emission. The solution to the difference is not now clear.

4.8 δ *vs.* Beam Current

It is well established that for metals the secondary current is proportional to the bombarding current over a wide range. With semiconductors and insulators the proportionality has sometimes been in question. With the targets studied here there has never been any serious departure from constancy of δ with varied beam current. Figure 15 reproduces one such run, where δ was constant within experimental errors over a range of more than 100:1 in beam current. The target was here at an intermediate temperature where the charging effect was small even at the larger currents.

4.9 δ *vs.* Primary Voltage

The maximum yield per primary electron comes at V_p about 1200 volts. In Fig. 16 are

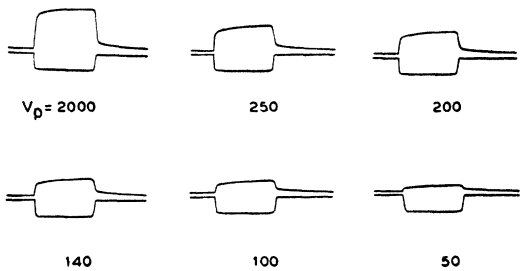

FIG. 14. Variation of enhanced emission with primary voltage. $i_p=17$ μa; $T=750°C$; $t=3$ μsec.

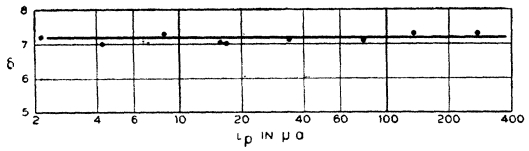

FIG. 15. Dependence of δ on beam current i_p. $V_p=1250$; $T=500°C$.

given curves A, B, and C of δ *vs.* V_p for three different temperatures, the one at 710°C being in the range where the thermionic contribution is considerable. The temperature variation is, in general, in accord with the data of Fig. 11.

It would be of interest to follow the curves beyond 2000 volts where Pomerantz finds a rapid decrease of δ, but this has not yet been done for reasons of insulation.

V. BARIUM POISONING

It is well known that the secondary emission of insulating or composite layers decreases with time when they are exposed in line-of-sight to a hot oxide cathode. Jonker and Overbeck,[9] for instance, discussed the effect in connection with targets of MgO. They assumed that deposition of metallic barium which evaporated from the oxide cathode[10] is responsible and took steps to avoid it by geometrical means.

The effect is very evident in the present tubes and has been given some consideration. When the target is heated for a short while to 700–800°C and cooled again to room temperature, curves of the form of curve A in Fig. 16 are obtained. All of the room temperature data shown so far have been obtained with the target thus relatively freshly cleaned. If now the target is exposed to the hot gun cathode for some hours the secondary yield decreases continuously. Curve D in Fig. 17 gives the secondary yield from the cold oxide target in the "poisoned" state. During the poisoning process there is no bombardment of the target and all but the gun heater voltage is turned off. The poisoning and cleaning processes seem not to depend on the presence of electric fields. When the entire system is turned off at any time during the poisoning cycle, the value of δ remains the same for a period of at least many days.

The variation of δ as the poisoning proceeds is shown by the series of photographs in Fig. 17. Here the gun cathode was continuously at operating temperature but the rest of the system was turned on only for a few minutes at a time to make the exposures. The secondary pulses look very much like the earlier ones in Fig. 8 where the target temperature was varied. Obviously δ decreases with time, and here, as in Fig. 8, the changing shape of the pulse indicates successively decreased resistivity of the oxide coating. In these respects the effects of barium poisoning are very similar to those of increasing temperature of the target.

The data of Fig. 18 show the time variation more clearly for three separate runs, where δ is plotted against time on a logarithmic scale. The target was started in the clean condition. At the end of the first run certain operations to be described were done, and the target was cleaned off for the second run. A single point marks the end of a third run of 6 hours after another clean-off. It is seen that in a period of 6 hours δ changed from about 12 to about 5 and would doubtless have reached a final value somewhat lower than this.

With this large change in δ one might expect also a change in work function of the oxide target. A number of attempts have been made to measure the change in work function, but they have been not entirely conclusive. The following is one of the best. The target was heated at 800°C for an hour and then let come to room temperature overnight. Then the target heater

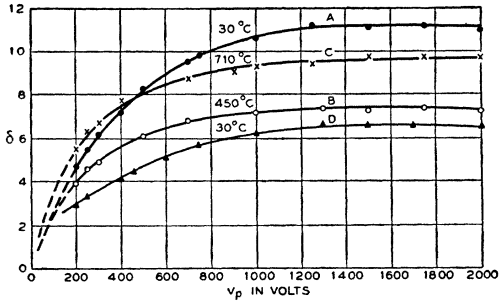

FIG. 16. Variation of δ with temperature, primary voltage, and poisoning. $i_p=8.5$ μa. A, B, C—clean target at 30°, 450°, and 710°C. D—poisoned target at 30°C.

[9] J. L. H. Jonker and A. J. W. M. v. Overbeck, W. Eng. 15, 150 (1938).
[10] J. A. Becker, Phys. Rev. 34, 1323 (1929).

was turned on and set to arrive at a final temperature of 305°C. The thermionic emission was measured once per minute, and after 15 minutes had reached the equilibrium current of 0.050 μa, representing the emission of the clean target. Now, after room temperature had again been reached, the second run of Fig. 18 was made ending at $\delta=6$. With the target in the poisoned state a second thermionic run was made in the same way, with the final emission 0.044 μa. At the end of this run with the target at 305° for half an hour the δ was measured again at room temperature. It had increased to 8.8 from 6.0 as a result of this low temperature heating, to the point of about 1-hr. poisoning. If it is assumed that the change of emission from 0.050 μa to 0.044 μa is caused by a change of work function of the target, then this change is given by

$$\Delta\varphi=\frac{2.3}{11600}T\log_{10}\frac{i_1}{i_2}=+0.005 \text{ ev.}$$

The same change of emission could also have been caused by the target temperature being lower in the second run by 1.5°. It is doubtful that the target heater could be set closer than this. Certainly no radical change in work function accompanies the change in δ from 12 to 8.8.

Secondary yield from metallic targets is known to vary with work function,[11] according to theoretical expectations,[12] but the variation is not rapid. Here the converse situation exists: large change in secondary emission and inappreciable change in work function. Some other factor than work function must here be responsible for the change in secondary yield.

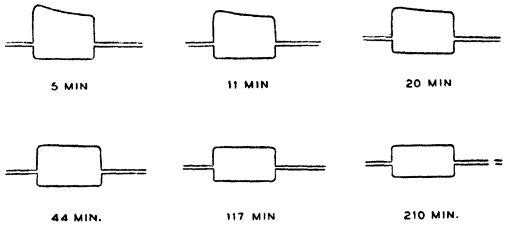

FIG. 17. Poisoning cycle. Exposure to gun cathode for various times. $t=10$ μsec.; $i_p=8.5$ μa; $V_p=1250$.

[11] K. Sixtus, Ann. d. Physik **3**, 1017 (1929); K. G. McKay, Phys. Rev. **61**, 708 (1942).
[12] D. E. Wooldridge, Phys. Rev. **56**, 562 (1939); J. H. deBoer and H. Bruining, Physica **6**, 941 (1939).

The most obvious explanation for the change in δ is that material evaporates from the gun cathode and settles on the target. Data in the files of these Laboratories indicate that the evaporated material is predominantly metallic Ba, and that at normal thermionic operating temperature and before long aging the evaporation rate is a maximum of the order 0.1 μg/cm^2 hr. The gun cathode, with the same type of coating material and base as the cathodes used in these evaporation tests, is run at a low temperature and can be assumed to have no greater evaporation rate than the figure quoted. The amount of Ba deposited on our target in a run will be estimated on the basis of this figure.

Examination of the tube structure, Fig. 1, shows that practically all of the emitting surface of the gun cathode "sees" a part of the target and all of the target "sees" the emitter through the disk apertures. Therefore, all of the evaporated material that reaches the apertures falls more or less uniformly on the target. Let S be the area of the emitter (0.80 cm^2), s the area of the target (0.317 cm^2), σ the area of the aperture (0.057 cm^2), and r the distance from emitter to aperture (1.46 cm). Let E be the rate of evaporation from the emitter (1×10^{-7} g/cm^2 hr.). Then, if the evaporation is uniform in all directions, the rate of arrival of material at the aperture from an element dS of the emitter is approximately

$$dW=E(\sigma/2\pi r^2)dS,$$

where $2\pi r^2$ is the area of the hemisphere about dS with radius r. From the whole emitter the rate is very nearly, per unit target area,

$$\frac{W}{s}=E\frac{\sigma S}{2\pi r^2 s}=1.08\times10^{-9} \text{ g/cm}^2 \text{ hr.}$$

The mass of the Ba atom is 2.3×10^{-22} g. The rate of deposit is therefore

$$W/s=0.47\times10^{13} \text{ atoms/cm}^2 \text{ hr.}$$

BaO crystallizes in the rocksalt structure with lattice spacing 5.5×10^{-8} cm. If we assume that the mixed oxide has the same lattice spacing and presents a smooth (100) plane, then the density of O atoms in this plane is

$$3.3\times10^{14} \text{ O atoms/cm}^2.$$

If each of these oxygen atoms were to adsorb one Ba atom for a monatomic layer of Ba, then the deposition of one layer would require 70 hrs. The actual surface of the target is, of course, much greater than 0.317 cm² and the density of adsorbed atoms correspondingly less. In the 6 hrs. of the longest poisoning run certainly much less than 0.1 monatomic layer was thus deposited on the target, and yet δ changed from 12 to 5.

It may be that the Ba does not remain on the surface but is absorbed into the lattice of the oxide, even at room temperature. The density of massive (BaSr)O should be 5.4. On the target is a layer 0.002 cm thick of density 1.27, so that the corresponding thickness of massive oxide would be

$$\tau = 4.7 \times 10^{-4} \text{ cm}.$$

After 6 hrs. of evaporation a cm² of this layer would have 2.85×10^{13} Ba atoms absorbed, or

$$0.6 \times 10^{17} \text{ Ba atoms/cm}^3.$$

This concentration of barium atoms, though not high, would affect the conductivity of the coating in the observed direction, and would be more likely to influence the secondary yield than the corresponding surface layer.

Evaporated metal atoms are known to have some mobility when condensed on a surface, tending to aggregate into small crystals. Yet it does not seem plausible that the Ba atoms can diffuse throughout the whole thickness of the coating at room temperature. If they migrate into a layer a few atoms deep, or the depth to which the primary electrons penetrate, then a considerable conductivity would be developed in this layer on top of the major insulating part of the coating. The surface charge could then spread to occupy a much larger area than the bombarded spot, affecting the induced surface potential in the same way as a larger body conductivity. This would delay or prevent the approach of the surface potential to that of the collector and so reduce the charging effect. At the same time the secondary emission would come largely from this more conducting part of the coating and could well be smaller than that of the more insulating oxide, in accordance with the variation of δ with temperature in the low temperature range.

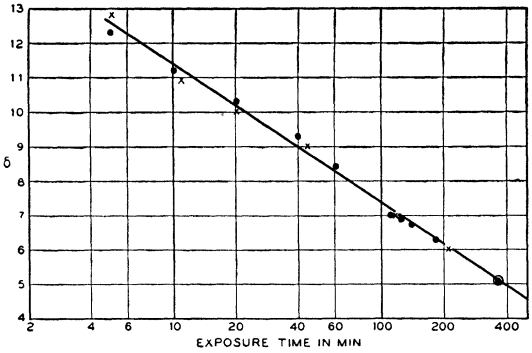

FIG. 18. Effect of exposure to gun cathode. $V_p = 1250$; Room temperature; three runs.

VI. THE POINT OF UNITY YIELD

At low values of bombarding voltage the yield as observed on the 'scope is illustrated by Fig. 19. The target is clean and at room temperature, and the curve should join curve A of Fig. 16. It is seen that δ passes through unity at about 27 volts, reaches a minimum at 7 volts, and then increases toward unity again as V_p is lowered. The values of δ are probably not very accurate over most of this range because the primary and secondary currents are not measured under nearly identical conditions in this region where V_c may be larger than V_p. Indeed, the observed δ varies considerably with V_c at low V_p.

At one point, however, where $\delta = 1.0$, the value of V_{p1} can be determined quite accurately. This is the value of V_p where the secondary deflection D_s is neither positive nor negative and the trace on the CR screen is straight with only slight kinks to mark the beginning and end of the pulse. V_{p1} can be set well within 0.1 volt for this condition with constant V_c. (Increasing V_c decreases V_{p1} because of incomplete saturation of i_s.) In this case D_p need not be measured separately, eliminating one source of error. Furthermore, there is then no net current through the coating and therefore no iR drop to consider; the face of the coating is at the same potential as the base plate.

In Fig. 20 is shown a series of values of V_{p1} for the clean target over a range of temperatures. At high temperatures the value is surprisingly low. With the "poisoned" target the values go to 35–40 volts at room temperature.

VII. ENERGY DISTRIBUTION OF THE SECONDARIES

In a gas with Maxwellian distribution of velocities of the molecules, the fraction of molecules having energy greater than a given amount E independent of direction of travel is given by[13]

$$f_c=\left(1+\frac{E}{kT}\right)e^{-(E/kT)}.$$

For thermionic electrons, a distribution curve of this type is obtained if the electrons come from a small central electrode surrounded by a large concentric sphere as collector, on which is applied the retarding potential E. The curve has a point of inflection where its derivative is highest, indicating the most probable energy of emission which in this case is greater than zero.

The central field method of retarding potential measurements has been much used because of its simplicity. The derivative of the curve gives the energy distribution even if the distribution is not Maxwellian. If, on the other hand, the electrodes have a planar structure, the retarding potential method does not give the total energy but only the energy corresponding to one of the three components of velocity. The equation is, for Maxwellian distribution,

$$f_x=e^{-(E_x/kT)}.$$

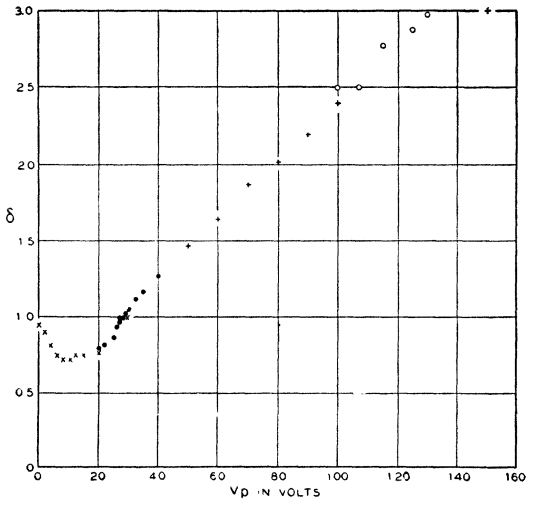

FIG. 19. Yield at low V_p—clean target, room temperature, four runs.

[13] J. H. Jeans, *Dynamical Theory of Gases* (The Cambridge University Press, New York, 1925), Section 28.

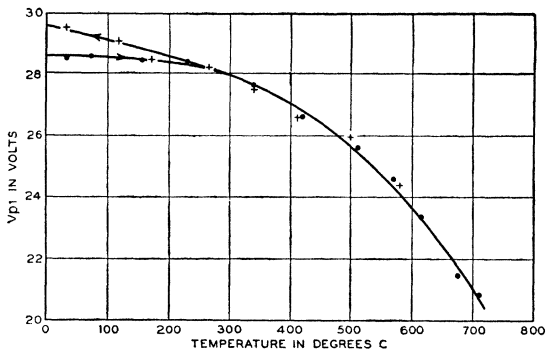

FIG. 20. Variation of V_{p1} with target temperature. Potential at which $\delta=1.0$, with rising and falling temperature.

It has no point of inflection and its derivative is a maximum when the velocity component is zero. Retarding potential measurements on the planar structure are therefore ill-suited for giving information on the total energy distribution of electrons.

The structure of target and collector in the present tube is far from either of these simple systems. On the other hand, both Pomerantz and Morgulis and Nagorsky have published curves obtained with structures no more suitable, and concluded from these that the average energy of the secondaries decreases with increasing temperatures. For a comparison, some retarding potential curves have therefore been run on our tube.

In these measurements the target was bombarded with electrons at 1250 volts, the beam current being made so small that the secondary current was only a fraction of a microampere in order to keep down space charge and iR drop. The beam current was steady and the secondary current was measured by a sensitive d.c. meter. Potential in the range of -25 to $+25$ volts was applied to the collector. Figure 21 shows a set of results, the secondary current being plotted against collector voltage. The change of voltage scale at -5 and $+5$ volts is to be noted. For curve a the target was at room temperature, while for curve b it was at 305°C. In the latter case there was a slight thermionic emission, observed separately in the absence of bombarding current and plotted as curve c. This curve gives the contact potential difference, the collector being obout 0.8-volt negative with respect to

the target. The difference between curves *b* and *c* is plotted as curve *b'*, representing the secondary current alone at the higher temperature. In the region to the left of +0.8 volt there is no significant difference between curves *a* and *b'* for the two temperatures. The curves are not differentiated in the usual way, for reasons already discussed, but their close coincidence suggests that there is here no appreciable change in energy distribution between room temperature and 305°C.

A similar set of curves is shown in Fig. 22 for the higher temperature 380°C. Here the thermionic emission is large instead of small compared with the secondary emission. Curve *a* is for room temperature as before, curves *d* and *e* are the total and thermionic emissions, plotted on a compacted current scale, and curve *d'* is the secondary current given by the difference between *d* and *e*, plotted on the original scale. To the left of the origin there is again no significant difference between curves *a* and *d'*. Any difference caused by a change in energy distribution must lie to the right in the region where a comparatively large thermionic current flows from which the secondary current cannot accurately be separated.

Finally, for comparison with the oxide target, an uncoated Ni target was used in a tube of similar structure, MN-1. A set of δ *vs.* V_p measurements for this target is shown in Fig. 23 for room temperature and an estimated 800°C. There is no appreciable change in δ over this temperature range, and the maximum δ occurs at about 500 v, in conformity with the usual results for metallic targets. That the target is not a clean metal surface is indicated by the value of $\delta=2.2$, which is too high for a clean

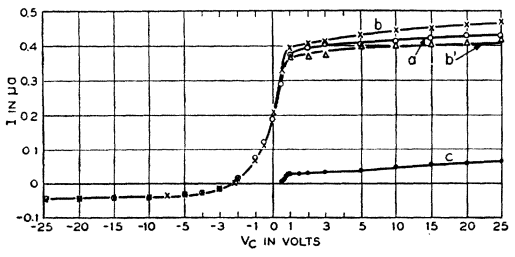

FIG. 21. Retarding potential curves. Thermionic current smaller than secondary current. $V_p=1250$; *a*, $T=30$°C; *b*, $T=305$°C; *c*, Thermionic, $T=305$°C; $b'=b-c$. Change of scale at −5 and +5 volts.

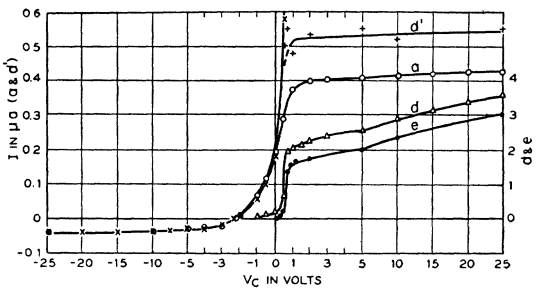

FIG. 22. Retarding potential curves. Thermionic current larger than secondary current. $V_p=1250$; *a*, $T=30$°C; *d*, 380°C; *e*, thermionic, $T=380$°C; $d'=d-e$.

metal. The best available information is that nickel has a δ_{max} of 1.3 at 550 volts.

The retarding-potential curve for this target is shown in Fig. 24, curve *II*, in comparison with curve *I* for the oxide target. The thermionic curve *III* for the nickel target indicates a contact potential of about 1 volt. While neither of the secondary curves gives a true energy distribution, the difference between the curves is very striking. Evidently the secondary electrons from the oxide have on the average a much lower energy of emission than those from the metallic target. Among the former only a small fraction is not stopped by −5 volts, while among the latter a larger fraction is not stopped by −25 volts. (This would make the observed δ for Ni too large, by indicating too small a primary current.) We can conclude, then, that while we do not know the exact energy distribution of the secondary electrons from the present oxide coating, their average energy is considerably below that for the metal, and that this distribution does not here change much in the temperature range where the secondary current is not swamped by thermionic current.

The assumption that the pulsed yield is all true secondary emission even at high temperatures here meets difficulties. The yield has been extrapolated by Pomerantz from values measured below 600°C to the thermionic operating temperature of 850°C, where it may be 100 secondary electrons per 1000-volt primary electron. This means that an incredibly large part of the primary energy goes into energy of the secondary electrons unless the energy of the latter is unusually small at the higher temperatures. Pomerantz considers the difficulty resolved in his finding (and that of Morgulis and Nagorsky)

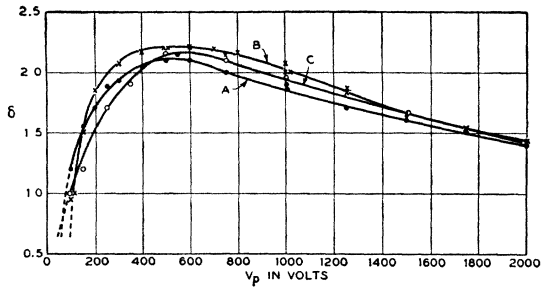

FIG. 23. Tube MN-1, Ni target, $i_p = 10.6\ \mu a$. *A*—room temperature; *B*—~800°C; *C*—room temperature.

that the secondary energy does decrease fairly rapidly with increasing temperature. This conclusion rests on the shape of energy distribution curves obtained by differentiating rather crude retarding-potential curves obtained with apparatus not suitable, as discussed above, for determining total energy distribution.

Other literature on the energy distribution of secondary electrons from insulators is also quite confusing. In some cases the experimental procedure has been faulty, leading to contradictory results. Treloar[14] working with composite CsO layers *predicted* for these a lower energy of secondary electrons than for metals. For NaCl Vudinsky[15] concluded that the energy distribution curves are similar to those for metals with a peak at possibly 3 to 6 volts. Kalckhoff[16] found for glass and mica the secondary energy peak at 15–20 volts and seemed not surprised. Malter[17]

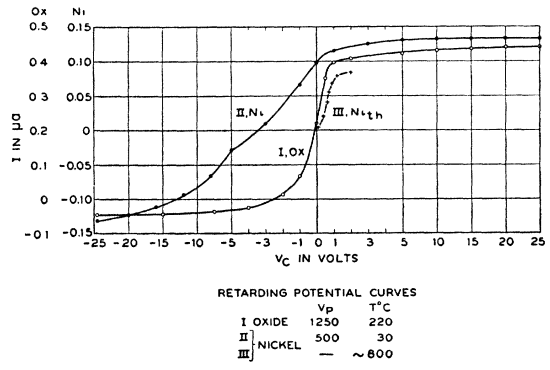

FIG. 24. Retarding potential curves. Nickel target compared with oxide target.

[14] L. R. G. Treloar, Proc. Lond. Phys. Soc. **49**, 392 (1937).
[15] M. Vudinsky, J. Tech. Phys. U.S.S.R. **9**, 1583 (1939).
[16] G. Kalckhoff, Zeits. f. Physik **80**, 305 (1932).
[17] L. Malter, Proc. I.R.E. **29**, 587 (1941).

obtained for Mg-Ag alloy (presumably oxidized) the most probable energy of emission of secondary electrons at 2–6 volts. For MgF_2 in thin layers Geyer[18] gives a distribution curve with the peak energy below his curve for Ni (2 volts), and similar layers of NaCl are not much different from the Ni curves. His insulator curves, however, show signs of an iR drop in the coating ("negative energy").

VIII. EFFECT OF HIGH FIELD ON SECONDARY EMISSION

In some instances when the target is poorly conducting there is seen a rising initial top portion of the secondary pulse. In Fig. 6b, for instance, there is a distinct rise during the first quarter-microsecond. A ready explanation is that as the surface becomes positively charged the internal field aids electrons in getting out and so increases the yield.[5] One might propose this as a major factor in making the δ of insulators high at low temperatures.

Some simple computations make this explanation less plausible. In the present targets the surface potential may reach at most that of the collector, say 60 volts. If this is distributed as a uniform field through the target, it would amount to about one millivolt per atomic layer of the oxide. It seems hardly reasonable that this small field could appreciably affect the motion of an internal secondary electron with energy of several electron volts. On the other hand, a field might be concentrated in a thin layer near the surface, say over the depth which the primary electrons reach, caused by the primaries being trapped at this depth while secondaries leave the surface. In order to get a significant field strength, say 0.1 volt per atomic layer, the charge delivered by the beam in the first quarter-microsecond in Fig. 6b should have been about 500 times what it actually was. It seems difficult to explain the initial rising top of the secondary pulse for the cold target on the basis of internal fields with the simple distribution assumed here. More needs to be known about the effect of field on the motion of internal electrons.

[18] H. K. Geyer, Ann. d. Physik **41**, 117 (1942).

IX. ACCURACY OF THE δ-MEASUREMENTS

The question was raised near the beginning of the article whether a retarding potential of 22 volts is sufficient to prevent all the secondaries from leaving the target so that an accurate measure can be made of the primary current. The retarding-potential curves, such as that of Fig. 21, seem to answer in the affirmative, having a very flat tail at the left in the retarding potential region. On the other hand, it is well recognized that secondary electrons have energies distributed all the way up to the primary energy. If in Fig. 21, 20 percent of the secondary electrons had energy near the primary energy the curve could still be as flat as it is now at -25 volts. The high speed secondaries would then in part strike the collector and there give rise to tertiary electrons which would be drawn to the target and measured as primary current. Similar errors, but not quite so large, apply to measurement of the secondary current. This confusion applies to practically all δ-measurements made by retarding-potential methods and makes the values of δ somewhat uncertain. It is never possible to draw unassailable conclusions about the origin of the various currents measured. This is why the retarding potential was specified in the definition of δ for the present measurements. A study of the few published reports on the ratio of high speed to low speed secondaries for various materials, and measurement in a few cases of currents to all the electrodes in the present work, suggests that 20 percent may be an upper limit to the errors in δ in the present measurements, introduced largely by the uncertainty in the measurement of primary current.

X. ACKNOWLEDGMENT

The author wishes to express his gratitude to many of his colleagues for valuable discussions during the progress of this work, in particular to Dr. K. G. McKay and Dr. Conyers Herring.